

Journal homepage: <https://modernpathology.org/>

Research Article

Clear Cell Stromal Tumor of the Lung: Clinicopathologic, Immunohistochemical, and Molecular Characterization of Eight Cases

Igor Odintsov^a, Alexandra Isaacson^b, Karen J. Fritchie^b, Yin P. Hung^c, Pooria Khoshnoodi^d, Lynette M. Sholl^a, Christopher D.M. Fletcher^a, William J. Anderson^{a*}

^a Department of Pathology, Brigham and Women's Hospital and Harvard Medical School, Boston, Massachusetts; ^b Department of Pathology, Robert J. Tomsich Pathology and Laboratory Medicine Institute, Cleveland Clinic, Cleveland, Ohio; ^c Department of Pathology, Massachusetts General Hospital and Harvard Medical School, Boston, Massachusetts;

^d Department of Pathology and Laboratory Medicine, University of Vermont Medical Center, Burlington, Vermont

ARTICLE INFO

Article history:

Received 8 July 2024
Revised 30 September 2024
Accepted 6 October 2024
Available online 16 October 2024

Keywords:

immunohistochemistry
mesenchymal
pulmonary
TFE3
YAP1

ABSTRACT

Clear cell stromal tumor is a recently described mesenchymal neoplasm of the lung, characterized by spindle cells with variably clear-to-pale eosinophilic cytoplasm and prominent vascularity, as well as a recurrent YAP1::TFE3 gene fusion in most cases. Diagnosis can be challenging given its rarity and the lack of supportive immunohistochemical (IHC) markers aside from TFE3. To date, less than 20 cases have been reported, and data on clinical behavior are also limited. Although most appear to be benign, aggressive behavior has been reported rarely. In this study, we present the largest multi-institutional series of clear cell stromal tumor to date, comprising a total of 8 cases and including 6 previously unpublished cases. We investigate its clinicopathologic and genomic features, while also assessing the diagnostic use of IHC for YAP1 C-terminus. Five patients were men and 3 were women. The median age was 59 years (range: 35–84 years). In all cases, a TFE3 rearrangement was demonstrated by either fluorescence in situ hybridization or DNA/RNA sequencing. In 7 tumors, the YAP1::TFE3 fusion was identified by sequencing. We demonstrate that the combination of YAP1 C-terminus loss and TFE3 overexpression using IHC reliably predicts an underlying YAP1::TFE3 fusion in these neoplasms and may be more sensitive than TFE3 fluorescence in situ hybridization. Although the median follow-up time for our study was short (18 months, available in 7 cases), all cases pursued a benign clinical course, with no recurrences or metastases. Our study provides further characterization of this novel entity, supporting its wider recognition.

© 2024 United States & Canadian Academy of Pathology. Published by Elsevier Inc. All rights are reserved, including those for text and data mining, AI training, and similar technologies.

Introduction

Clear cell stromal tumor (CCST) of the lung is a recently described distinctive pulmonary mesenchymal neoplasm characterized by spindle cells with variably clear or palely eosinophilic

cytoplasm and a recurrent YAP1::TFE3 gene fusion. It was first described in 2013 by Falconieri et al¹ in a report of 2 cases. The authors used the provisional term "hemangioblastoma-like clear cell stromal tumor of the lung," as the clear cell cytomorphology, prominent vascularity, and variably nested growth pattern were together considered reminiscent of hemangioblastoma.¹ Despite this, no mutations in the coding sequence of VHL were identified in the 1 profiled case. Both cases were negative for epithelial, melanocytic, muscular, and neuroendocrine markers, and only focal CD34 staining was observed. Subsequently, Lindholm and

This work was presented in part at the 113th Annual Meeting of the United States and Canadian Academy of Pathology, March 2024 (Baltimore).

* Corresponding author.

E-mail address: wanderson@bwh.harvard.edu (W.J. Anderson).



Moran² reported an additional 5 cases and further attempted to establish the line of differentiation using immunohistochemistry (IHC). Notably, apart from vimentin, the tumors were negative for all the markers performed, including cytokeratins, epithelial membrane antigen (EMA), TTF-1, p40, chromogranin, synaptophysin, CD34, CD31, STAT6, desmin, smooth muscle actin (SMA), GATA3, S-100 protein, SOX10, and HMB-45. These results echoed the earlier findings of Falconieri et al.¹ who also found no reliable IHC marker for these neoplasms.

An important breakthrough in our understanding of the pathogenesis of CCST came in 2021, when Agaimy et al.³ demonstrated the recurrent *YAP1*:*TFE3* fusion in 5 of 6 cases. Later that year, Dermawan et al.⁴ corroborated this finding in their report of 2 cases that harbored the same fusion. These studies have helped to establish CCST as an emerging entity and facilitate its diagnosis using molecular methods to demonstrate *TFE3* rearrangements or *YAP1*:*TFE3* fusions and/or *TFE3* IHC. In recent years, additional cases of CCST have also been reported by Dehner et al.,⁵ Jaksa et al.,⁶ and Zhang et al.⁷ Nevertheless, to date, only 19 cases have been reported, and CCST is yet to be incorporated into the World Health Organization Classification of Thoracic Tumors.

Diagnosis of this rare tumor without molecular testing remains challenging, partly because, as outlined above, CCST is negative for most IHC markers and positive staining is usually limited to nuclear expression of *TFE3*. Although the latter is certainly helpful to support the diagnosis, variable *TFE3* expression can be observed in several other tumor types, such that positivity for *TFE3* alone is not entirely specific.⁸ In other neoplasms harboring *YAP1* fusions, such as the *YAP1*:*TFE3*-rearranged variant of epithelioid hemangiopericytoma⁹ and *YAP1*-rearranged poroma and porocarcinoma,¹⁰ IHC for *YAP1* C-terminus (*YAP1*-CT) can be diagnostically helpful. Typically, such tumors show loss of expression of *YAP1*-CT, likely related to the disruption of *YAP1* caused by rearrangement and the fact that only the N-terminal region of *YAP1* is retained in the oncogenic fusion proteins. We, therefore, hypothesized that IHC for *YAP1*-CT may also be useful in the diagnosis of CCST and offer additional specificity when used alongside *TFE3*.

In addition to the diagnostic challenge of CCST, its biologic potential is still not entirely understood given the relatively small number of cases in the literature with long-term follow-up. Although most cases have followed a benign clinical course, one of the patients reported by Dehner et al.⁵ presented with metastases and died of the disease. Furthermore, in the study of Agaimy et al.,³ 1 patient presented with multiple metastases involving the kidneys and liver, and a second patient demonstrated metastatic involvement of the hilar lymph nodes that were removed with pneumonectomy. These more aggressive cases support that more information is required to better characterize the clinical behavior of CCST.

In this multiinstitutional study of CCST, the largest series to date, we present the clinicopathologic, IHC, and molecular features of 8 fusion-positive cases. In addition to further interrogating the genetic features of CCST using targeted DNA/RNA sequencing and fluorescence in situ hybridization (FISH), we investigate the use of *YAP1*-CT and *TFE3* as IHC surrogates for molecular testing. Clinical follow-up data are also presented to further characterize the biologic potential of this unusual neoplasm. Finally, separate to this cohort, we describe the features of a pulmonary neoplasm morphologically mimicking CCST and expressing *TFE3*, but showing retained *YAP1*-CT and lacking *TFE3* rearrangement.

Materials and Methods

This study was approved by the Institutional Review Board of Mass General Brigham (protocol number: 2023P002089). A total of 8 CCST cases were identified for inclusion in the study. Cases were retrieved from the departmental and consultation files of Brigham and Women's Hospital, including the consultation files of one of the authors (C.D.M.F.), as well as the archives of collaborating institutions (provided by A.I. and K.J.F.). Representative hematoxylin and eosin-stained slides, as well as available IHC stains of all cases were reviewed to confirm the diagnosis of CCST. Six cases had been initially diagnosed as CCST (cases 3–8). Two cases were identified on the retrospective review of previously unclassified neoplasms (cases 1 and 2). These were initially diagnosed descriptively as “benign spindle cell neoplasm with prominent inflammatory component” (case 1, diagnosed in 2009) and “atypical spindle and clear cell neoplasm” (case 2, diagnosed in 2015). Cases 3 and 6 were previously published by Dermawan et al.⁴ (as cases 1 and 2, respectively) and were included to provide additional follow-up information and to assess with *YAP1*-CT IHC. A ninth case, which had been prospectively diagnosed as CCST by one of the authors, was initially included in this study but ultimately excluded from the cohort since a definitive diagnosis of CCST could not be confirmed following an overall assessment of its morphologic, IHC, and molecular features (see section “Clinicopathologic and molecular features of pulmonary spindle cell neoplasm lacking *TFE3* rearrangement”).

IHC was performed on 4-μm-thick formalin-fixed paraffin-embedded tissue sections following pressure cooker antigen retrieval (Target Retrieval Solution, pH 6.1; Dako). The following antibody clones, dilutions, and sources were used: *YAP1*-CT (clone: D8H1X; 1:100; Cell Signaling Technology) and *TFE3* (clone: MRQ-37; 1:100; Cell Marque). Positive control slides were stained in parallel.

FISH to assess for *TFE3* rearrangement was performed on 4 tumors using homebrew break-apart probes specific for the 5' and 3' regions of *TFE3* at Xp11.23 and a probe for Xp11.1-q11.1 (DXZ1; Abbott Molecular). The schematic of the probe design is provided in Supplementary Figure S1.

OncoPanel targeted DNA sequencing was performed on 2 tumors using OncoPanel as previously described.¹¹ Supplementary File S1 includes a detailed description of the methodology and covered genes. Anchor-based multiplex PCR and next-generation RNA sequencing were performed on 5 tumors as previously described.¹² The following transcripts were used for the genes discussed in the “Results” section: *TFE3* NM_001282142.2, *YAP1* NM_001195045.2, and *FLCN* NM_144997.7. Supplementary File S2 includes covered genes. Genomic variants were reviewed in Broad Institute Integrative Genomics Viewer.¹³

Results

Clinical Features

The clinical features are summarized in Table 1. The cohort of *TFE3* rearrangement-positive CCST comprised 8 patients (5 men and 3 women) with a median age of 59 years (range: 35–84 years). Tumors occurred in the right upper lobe (n = 1), right middle lobe (n = 1), right lower lobe (n = 2), and left lower lobe (n = 3). For 1 tumor, occurring in the right lung, the precise location (ie, lobe) was not specified. One patient's tumor was detected on an annual low-dose chest computed tomography scan for lung cancer screening purposes. Serial imaging studies had

Table 1

Clinicopathologic features of clear cell stromal tumor

Case no.	Age (y)	Sex	Site	Size (cm)	Follow-up time (mo)	Outcome
1	42	Male	LLL	2.3	104	ANED
2	56	Female	RL	NA	NA	NA
3	77	Male	LLL	3.9	7	ANED
4	63	Male	RLL	2	3	ANED
5	84	Female	LLL	5.5	18	ANED
6	35	Male	RML	7.5	33	ANED
7	61	Female	RLL	0.7	3	ANED
8	41	Male	RUL	3.4	22	ANED

ANED, alive with no evidence of disease; LLL, left lower lobe; NA, not available; RL, right lung; RLL, right lower lobe; RML, right middle lobe; RUL, right upper lobe.

demonstrated a gradual increase in size from 4.5 to 6 mm in 3 years, and then from 6 to 7.5 mm in 1 year (Fig. 1A, B). Clinical follow-up data were available for 7 patients (median follow-up duration: 18 months; range: 3–104 months). No patients developed local recurrence or metastasis.

Pathologic Features

The histologic findings of CCST are summarized in Table 2. All tumors appeared as well-delineated round nodules (Fig. 1B). The median tumor size was 3.4 cm (range: 0.7–7.5 cm). Microscopically, the tumors involved conductive airways, frequently in proximity to a pulmonary artery branch. There was typically an apparent sharp interface at low power but, at higher power, the respiratory epithelium was present toward the periphery and lining, and occasionally invaginated the tumor nodule, imparting a biphasic appearance (Fig. 2). Distinctive thin-walled and/or staghorn-shaped vessels were present in all tumors (Fig. 3A). In all cases, the neoplastic cells formed focal polypoid projections

(Fig. 3B) within the lumen of thin-walled vessels. Five of 8 cases also demonstrated foci of intratumoral vascular thrombosis.

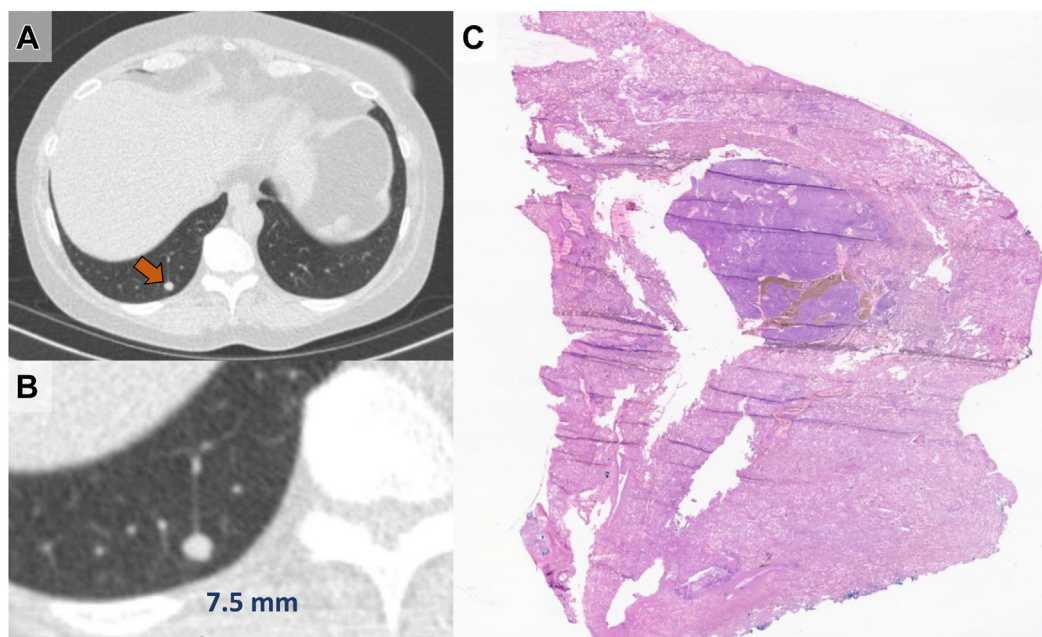
A chronic inflammatory cell infiltrate was characteristically present (Fig. 4). In all the cases, there was a predominantly lymphocytic infiltrate present as scattered cells and occasional small aggregates (Fig. 4A). In some tumors, the inflammatory infiltrate also included prominent eosinophils, whereas many tumors also demonstrated aggregates of foamy histiocytes (6/8 cases; Fig. 4B).

Cytomorphologically, the tumors were mostly composed of histiocytoid, ovoid- to spindle-shaped cells. Cell borders were typically indistinct, and the cells formed sheets with occasional loose nests and whorls. Despite the name CCST, clear cytoplasm was only a prominent finding in a minority of cases (Fig. 5). More commonly, the tumor cells exhibited variably clear and pale eosinophilic cytoplasm. The cells generally had relatively uniform nuclei with inconspicuous nucleoli and no significant atypia. However, bizarre nuclei with degenerative atypia were focally identified in most cases (7/8 cases; represented in Fig. 5G). These nuclei were large (characteristically, 3–6 times the size of the regular tumor cells) and showed irregular contours with occasional prominent nucleoli or smudgy chromatin. Mitotic activity was either absent or very low. Only 1 tumor demonstrated 3 mitotic figures per 2 mm.² No tumors had areas of necrosis.

A frozen section was performed on 1 tumor intraoperatively. The tumor retained most of its diagnostic features, including the presence of monotonously irregular ovoid- to spindle-shaped cells with indistinct cell borders growing in loose nests and frequent thin-walled vessels (Supplementary Fig. S2).

Immunohistochemical and Molecular Genomic Findings

The IHC and genomic findings are summarized in Table 3, and all additionally performed IHC are summarized in Supplementary File S3. All tumors demonstrated diffuse, homogeneous nuclear expression of TFE3 (Fig. 6A) and showed diffuse, homogenous loss

**Figure 1.**

Radiologic features and the intraoperative frozen section of a clear cell stromal tumor (case 7). (A, B) This asymptomatic patient underwent chest computed tomography screening owing to her significant smoking history. First imaging from 2019 demonstrated a 4.5-mm solid, round, well-defined nodule that grew to 6 mm in 2022 and 7.5 mm in 2023, when the patient underwent a lung wedge resection. (C) Low-power magnification of the intraoperative frozen section demonstrating a well-defined appearance.

Table 2

Summary of histopathologic features of clear cell stromal tumor

Case no.	Mitotic activity (per 2 mm ²)	Staghorn-shaped vessels	Lymphocytic aggregates	Polypoid projections	Bizarre nuclei	Entrapment of respiratory epithelium	Foamy histiocytes	Intratumoral thrombosis
1	3	+	+	+	-	+	+	+
2	<1	+	+	+	+	+	-	+
3	1	+	+	+	+	+	+	-
4	1	+	+	+	+	-	-	-
5	0	+	+	+	+	-	+	+
6	0	+	+	+	+	+	+	-
7	1	+	+	+	+	+	+	-
8	0	+	-	-	-	+	-	+
	100% (8/8)	88% (7/8)	88% (7/8)	75% (6/8)	75% (6/8)	63% (5/8)	50% (4/8)	

of expression of YAP1-CT (Fig. 6B-E). We confirmed the presence of *TFE3* rearrangement in all cases with nuclear *TFE3* expression and loss of YAP1-CT. In 7 of these cases, *YAP1* (exon 4)::*TFE3* (exon 7) fusion was identified using either DNA-based or RNA-based testing. In 1 additional tumor, *TFE3* rearrangement was demonstrated using FISH with break-apart probes, but the exact nature of the rearrangement could not be further specified as the sample failed RNA-based testing. Of note, 2 tumors that were positive for *YAP1*::*TFE3* fusion on DNA/RNA-based sequencing were falsely negative for *TFE3* rearrangement using FISH.

Clinicopathologic and Molecular Features of Pulmonary Spindle Cell Neoplasm Lacking *TFE3* Rearrangement

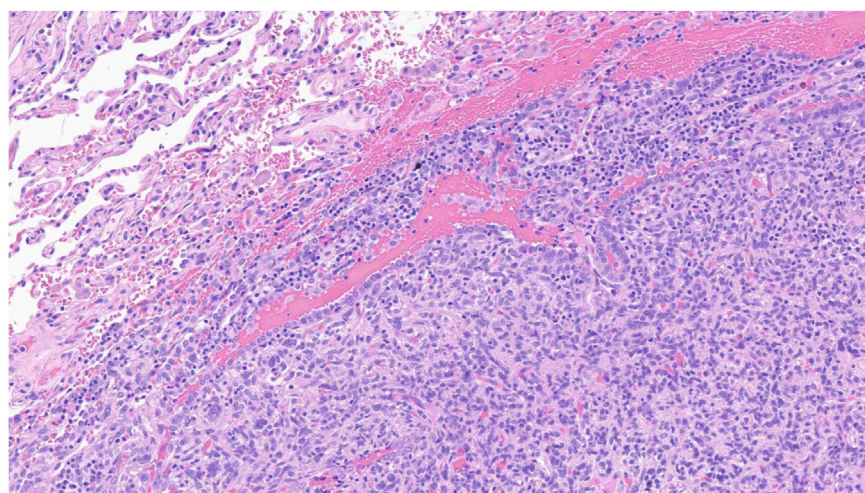
An additional (ninth) pulmonary spindle cell neoplasm that had been diagnosed prospectively as "CCST" based on its morphology and nuclear *TFE3* expression was initially included in the study; however, it demonstrated retained YAP1-CT expression (Fig. 7), and accordingly, no *TFE3* or *YAP1* rearrangements were detected using *TFE3* FISH, DNA-based sequencing, and RNA-based sequencing. As a definitive final diagnosis of CCST could not be confirmed, this case was excluded from the main cohort described above. Histologically, this tumor showed more regular nuclear contours, prominent nucleoli, and less-prominent infiltrating lymphocytes than the tumors classified as CCST (Fig. 5I). Analysis of the copy number data derived from DNA-based sequencing

demonstrated near haploidization with loss of almost all chromosomes except chromosomes 5, 16, 20, and 22. A review of the detected single-nucleotide variants uncovered a pathogenic nonsense mutation in *FLCN* p.W376*. Coupled with the loss of chromosome 17, this mutation is predicted to result in a biallelic loss of *FLCN* (Supplementary Fig. S3). This tumor was strongly and diffusely positive for cathepsin K, whereas it was negative for SMA, HMB-45, and Melan A.

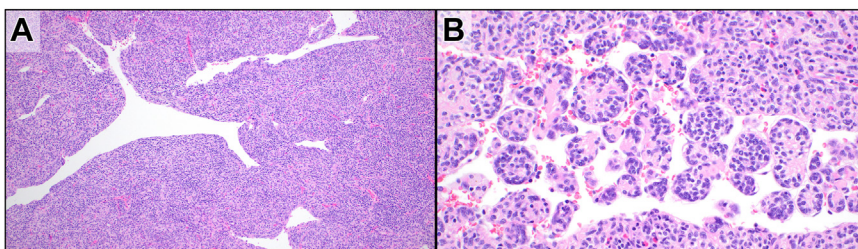
Discussion

CCST of the lung is a neoplasm of uncertain differentiation that represents an emerging entity. Most cases reported to date have followed a benign clinical course. In this study, we have presented further data supporting that these neoplasms more commonly follow an indolent course, as none of the 7 patients with available follow-up demonstrated recurrences or metastases. Nevertheless, it is important to note that one of the limitations of our study is the relatively short follow-up time (median: 18 months). It is important to keep in mind that rare examples of these neoplasms have been reported to present with regional lymph node metastases or distant metastases.^{3,5} Table 4 summarizes the clinicopathologic features, molecular findings, and outcomes of all previously published cases combined with our cohort.

At the genomic level, most CCST are characterized by a recurrent *YAP1*::*TFE3* fusion. Given the lack of specific IHC markers of

**Figure 2.**

A medium-power view showing the interface and overlaying and invaginating airway epithelium.

**Figure 3.**

Vascular features of clear cell stromal tumor. (A) Dilated, thin-walled, staghorn-shaped vessels were easily identifiable and were present in all cases. (B) Distinct polypoid tumor projections were present in 7 out of 8 cases.

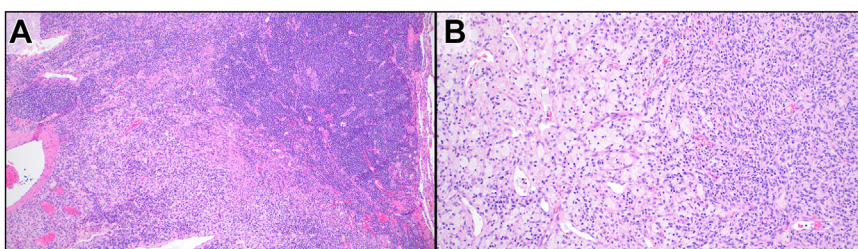
differentiation, diagnosis of CCST is commonly made on the combination of morphologic features, TFE3 IHC, and confirmation of *TFE3* rearrangement, either with FISH or with next-generation sequencing (NGS)-based methods. As the C-terminal portion of YAP1 is not expressed in the fusion protein, we hypothesized that loss of YAP1-CT staining can provide an accessible surrogate marker for YAP1 rearrangement in CCST. Indeed, we demonstrate that the combination of TFE3 and YAP1-CT IHC reliably predicts an underlying YAP1::*TFE3* fusion (7/7 cases).

Interestingly, 3 cases of CCST in our study that were found to harbor YAP1::*TFE3* fusion using NGS also underwent testing with break-apart *TFE3* FISH, yet a positive FISH result was only obtained in 1 out of 3 cases. These findings suggest that break-apart *TFE3* FISH could be inferior to the combination of TFE3 and YAP1-CT IHC or NGS assays in the diagnosis of CCST. Similarly, Agaimy et al.³ tested 3 cases with *TFE3* FISH and showed that FISH was falsely negative in at least 1 case with YAP1::*TFE3* fusion detected using RNA sequencing. Two other tested cases were concordant, which was as follows: 1 case was positive for *TFE3* rearrangement based on FISH and RNA sequencing and the other was negative based on both. The authors postulated that the falsely negative *TFE3* FISH result could be related to the FISH probe design. The reason for false-negative FISH in our cases remains unclear but does not appear to be related to probe design. Other factors that could possibly cause false-negative results include the presence of a prominent nonneoplastic inflammatory cell infiltrate in many cases and technical issues such as poor fixation and sectioning artifacts. Regardless, these findings suggest that a negative *TFE3* FISH result does not fully exclude the diagnosis of CCST as an underlying YAP1::*TFE3* fusion may still be present.

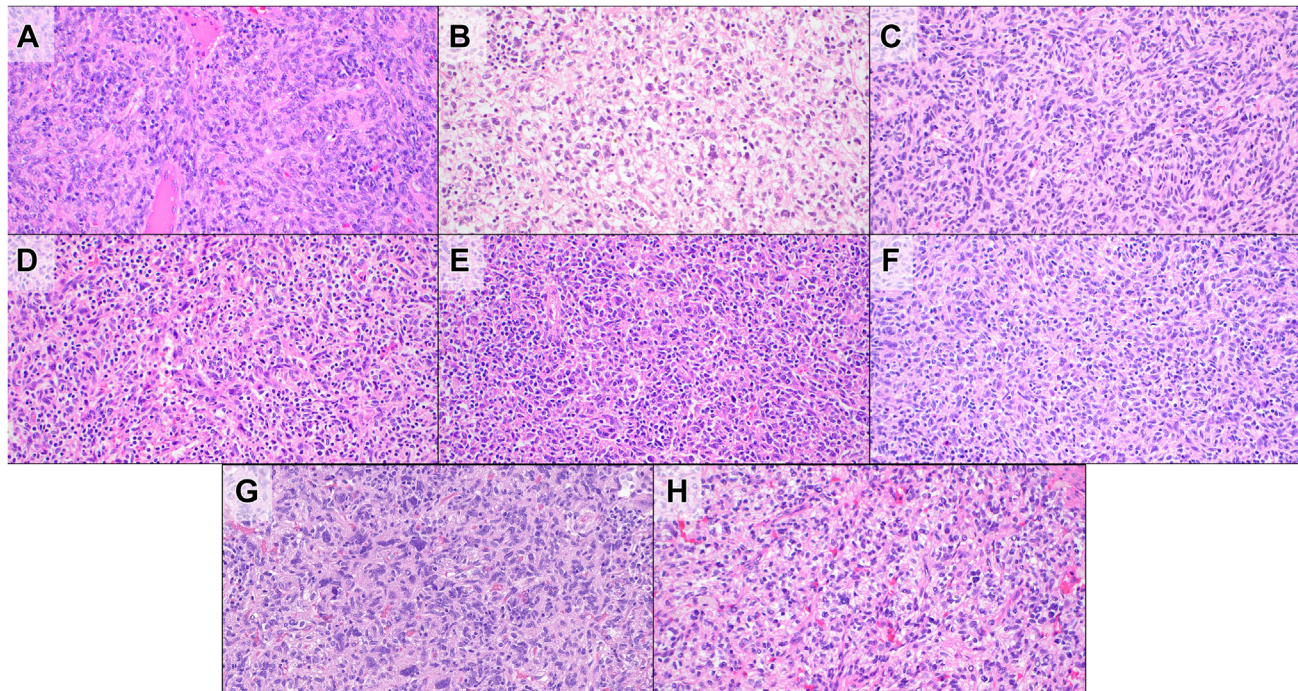
In our study, all YAP1::*TFE3* fusions demonstrated a consistent breakpoint resulting in a chimeric protein consisting of YAP1 exons 1 to 4 and *TFE3* exons 7 to 10. All previously reported CCST cases with available fusion data demonstrated identical breakpoints,³⁻⁶ with the exception of a single case that showed YAP1 exon 5::*TFE3* intron 6 fusion.³ In the YAP1 exon 4::*TFE3* exon 7

fusion, YAP1 contributes the TEAD-interacting domain, WW domains, and 14-3-3 protein-binding site, whereas the *TFE3* portion adds the basic helix-loop-helix domain, leucine zipper domain, and the C-terminal transactivation domain. Thus, the resulting chimeric oncprotein likely draws on the strength of both parent proteins and may evade some of the physiological negative regulation. Of note, the YAP1::*TFE3* rearrangement that occurs in the variant epithelioid hemangioendothelioma connects YAP1 exon 1 to *TFE3* exon 4 or 6.¹⁴ Interestingly, unlike the CCST fusion, this rearrangement lacks the 14-3-3 binding site S127. When phosphorylated, S127 creates a binding site for 14-3-3 that sequesters YAP1 to the cytoplasm and suppresses its nuclear activity.¹⁵ Retained regulation by 14-3-3 might explain the relatively indolent clinical course of CCST.

As in the series of Agaimy et al.,³ we also encountered 1 tumor with similar morphologic features to CCST and nuclear expression of TFE3, but that was negative for the YAP1::*TFE3* fusion (see section "Clinicopathologic and molecular features of pulmonary spindle cell neoplasm lacking *TFE3* rearrangement"). Instead, targeted DNA sequencing revealed a nonsense *FLCN* p.W376* mutation and findings suggesting biallelic inactivation. Folliculin, encoded by *FLCN*, is a tumor suppressor involved in regulating cell growth, metabolism, and the response to cellular stress.¹⁶ Under normal conditions, folliculin forms a complex with folliculin-interacting proteins 1 and 2 and activates mechanistic target of rapamycin complex 1. Activated mechanistic target of rapamycin complex 1, in its turn, phosphorylates TFE3 and TFEB, leading to their retention in the cytoplasm.¹⁷ Loss of folliculin is therefore postulated to result in translocation of TFE3 to the nucleus.¹⁶ In keeping with this, this tumor demonstrated moderate nuclear TFE3 signals on IHC and retained YAP1-CT. Nuclear activity of full-length TFE3 is known to stimulate autophagy and lysosome biogenesis.¹⁷ Accordingly, there was strong and diffuse expression of cathepsin K (a lysosomal cysteine proteinase). Of note, inactivating *FLCN* mutations have been reported in rare examples of perivascular epithelioid cell tumors (PEComas).¹⁸ Although this

**Figure 4.**

Inflammatory infiltrate. (A) Scattered individual lymphocytes were present in all cases, and 7 out of 8 cases demonstrated lymphoid aggregates that were most abundant at the interface with lung parenchyma. (B) Aggregates of foamy histiocytes were found in 5 out of 8 cases.

**Figure 5.**

Cytomorphologic features of the clear cell stromal tumor cohort. (A-H) Cases 1 to 8. Clear cytoplasm was predominant in only a minority of cases, and most tumors displayed only focal or no clear cytoplasm. (G) Bizarre nuclear atypia was present in 6 out of 8 cases. These nuclei were characteristically large (3-5 times the size of the regular tumor nuclei) and showed highly irregular nuclear contours, smudgy chromatin, and occasional cherry-red nucleoli with perinucleolar clearing.

differential diagnosis perhaps cannot be entirely excluded, the tumor was negative for melanoma markers (HMB-45 and Melan A) and muscle markers. Additional similar cases are required to determine if this tumor represents a variant of CCST or a biologically distinct neoplasm with similar morphology.

The differential diagnosis of CCST is broad and commonly includes solitary fibrous tumor (SFT), PEComa, hemangioblastoma, sclerosing pneumocytoma, pulmonary carcinoid, inflammatory myofibroblastic tumor (IMT), and angiomyomatoid fibrous histiocytoma (AFH). CCST may focally resemble hemangioblastoma, accounting for its prior designation as "hemangioblastoma-like clear cell stromal tumor."¹ Unlike true hemangioblastoma, however, CCST does not express S100 protein, neuron-specific enolase, or inhibin. Primary peripheral or metastatic hemangioblastomas are exceedingly rare in the lung, with less than 5 cases reported in English literature.¹⁹

The possibility of SFT is often raised by the intrathoracic location and frequent presence of prominent thin-walled staghorn-like vessels. CCST and SFT can also both comprise haphazardly arranged spindle cells with indistinct borders. However, in the thorax, SFT is more commonly pleural based, whereas CCST tends to occur within lung parenchyma and frequently in association with the airway epithelium. Occasionally, SFT can originate from pleural infoldings of an interlobar fissure, mimicking an intra-parenchymal appearance on chest imaging. In cases of small biopsies and unclear radiologic findings, IHC can readily aid distinction, as SFT is positive for STAT6 and negative for TFE3.

PEComa is another neoplasm that demonstrates similar morphologic features. PEComas are typically composed of cells with clear cytoplasm arranged in nests and cords. Radial, perivascular distribution can be seen in a minority of cases. Unlike CCST, PEComas commonly display well-defined cell borders. The

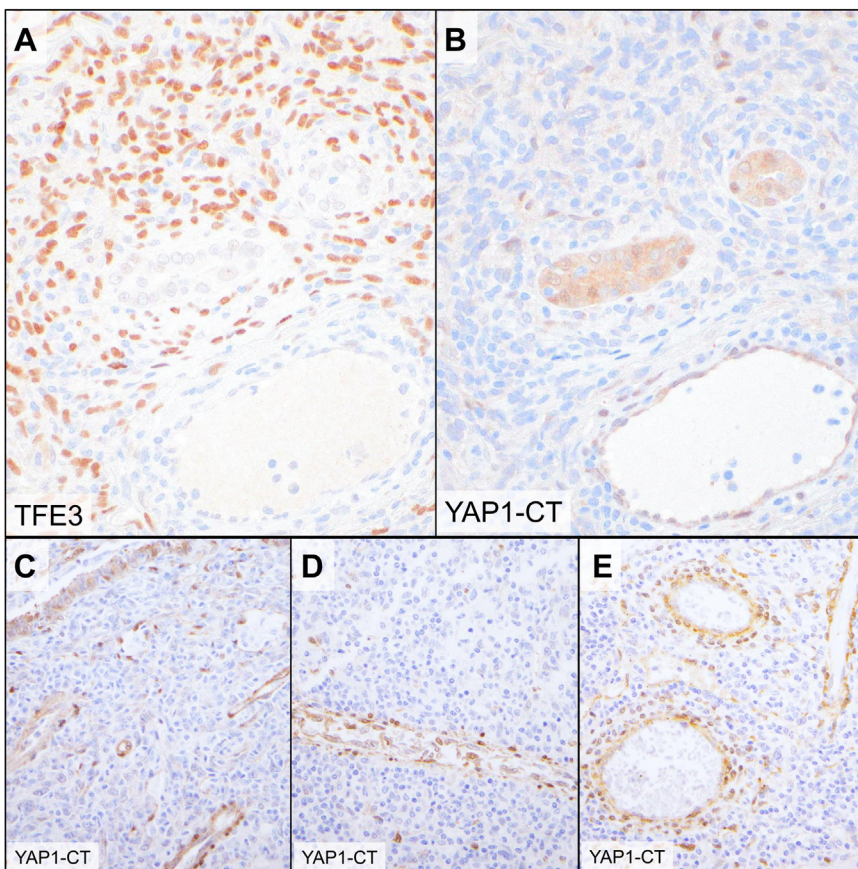
Table 3

A summary of molecular genomic features of clear cell stromal tumor

Case no.	Immunohistochemistry		TFE3 FISH	NGS
	TFE3	YAP1-CT		
1	POS	LOST	NP	YAP1 (exon 4)::TFE3 (exon 7) (targeted RNAseq)
2	POS	LOST	Negative	YAP1 (exon 4)::TFE3 (exon 7) (targeted DNAseq)
3 ^a	POS	LOST	NP	YAP1 (exon 4)::TFE3 (exon 7) (targeted RNAseq)
4	POS	LOST	NP	YAP1 (exon 4)::TFE3 (exon 7) (targeted RNAseq)
5	POS	LOST	NP	YAP1 (exon 4)::TFE3 (exon 7) (targeted RNAseq)
6 ^a	POS	LOST	NP	YAP1 (exon 4)::TFE3 (exon 7) (targeted RNAseq)
7	POS	LOST	Negative	YAP1 (exon 4)::TFE3 (exon 7) (targeted RNAseq)
8	POS	LOST	Positive	Failed RNAseq

DNAseq, next-generation tumor DNA-sequencing panel OncoPanel; FISH, fluorescence in situ hybridization; LOST, loss of expression; NGS, next-generation sequencing; NP, not performed; POS, positive; RNAseq, anchor-based multiplex PCR and next-generation RNA sequencing.

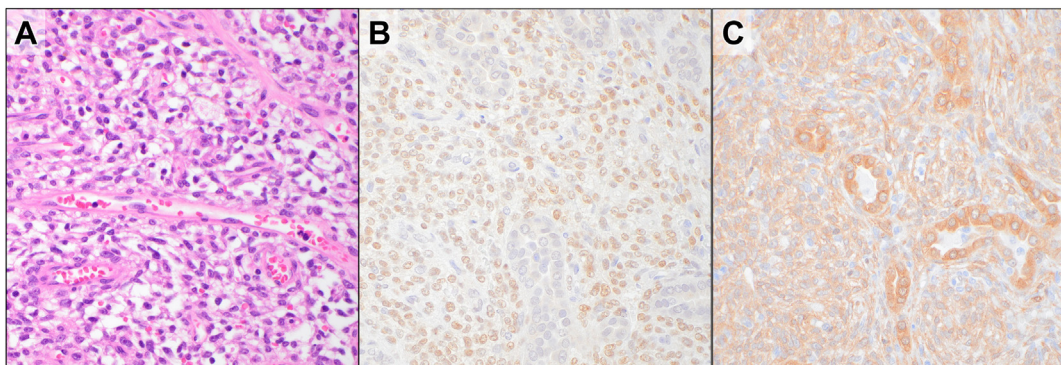
^a Previously reported by Dermawan et al.⁴

**Figure 6.**

Representative images of (A) TFE3 and (B-E) YAP1-CT immunohistochemistry in *YAP1::TFE3*-rearranged clear cell stromal tumor. Absence of TFE3 staining and retained expression of YAP1-CT in the entrapped airway epithelium and vascular endothelium serve as the internal control.

differentiation between CCST and PEComas is further complicated by the fact that TFE3 overexpression can be detected in PEComas as well, owing to *TFE3* translocations that can be seen in some of these tumors. Nevertheless, no reported *TFE3* translocations in PEComas affected *YAP1*.²⁰ YAP1-CT is therefore predicted to be retained in PEComas. Moreover, no cases of CCST so far have demonstrated expression of myomelanocytic markers such as SMA, HMB-45, Melan A, or MITF.

IMT is characterized microscopically by a mixed population of myofibroblast-like spindle cells and inflammatory cells. Extensive infiltration by chronic inflammatory cells in CCST can therefore mimic IMT. In contrast with CCST, the tumor cells in IMT are typically more spindled or stellate with eosinophilic cytoplasm and larger nuclei with open chromatin and conspicuous nucleoli. IMT most typically harbors translocations in *ALK* or *ROS1*, which can be

**Figure 7.**

Pulmonary spindle cell neoplasm lacking *TFE3* rearrangement. (A) The tumor was composed of ovoid-to-spindled cells arranged in sheets and vague nests. Dilated thin-walled vessels were present throughout the tumor. Lymphocytic infiltration was very sparse, compared to the cases classified as clear cell stromal tumor. On high power, the cells demonstrated clear cytoplasm and ovoid-to-spindle-shaped nuclei with regular nuclear contours and prominent nucleoli. Unlike most of the cases classified as clear cell stromal tumor, bizarre nuclear atypia was absent. (B) This tumor demonstrated weak-to-moderate nuclear TFE3 expression. (C) There was retained expression of YAP1 C-terminus.

Table 4

Reported cases of clear cell stromal tumor (25 cases)

Reference	Sex	Age (y)	Site	Size (cm)	Molecular findings	Outcome (follow-up duration)
Falconieri et al ¹	Female	68	RUL	6	NA	ANED (2 y)
	Male	40	LLL	3	No mutation in the coding sequence of <i>VHL</i> ; no other molecular testing	ANED, (2 y)
Lindholm and Moran ²	Female	46	RLL	2.8	NA	ANED (36 mo)
	Female	47	RUL	2	NA	ANED (20 mo)
	Male	52	LUL	2.5	NA	NA
	Female	39	RUL	2.5	NA	ANED (18 mo)
	Female	42	LLL	2	NA	NA
Agaimy et al ³	Female	56	LUL	2.3	<i>YAP1</i> (exon 4):: <i>TFE3</i> (exon 7)	ANED (36 mo)
	Female	29	Lung, not specified	9.5	<i>YAP1</i> (exon 5):: <i>TFE3</i> (intron 6)	NA
	Female	69	LUL	4	<i>YAP1</i> (exon 4):: <i>TFE3</i> (exon 7)	ANED (12 mo)
	Female	66	LMB	NA	Negative for <i>YAP1</i> :: <i>TFE3</i> fusion on RNAseq testing; negative for <i>TFE3</i> rearrangement based on FISH; <i>SETD2</i> p.G1581E on DNA sequencing	AWD (4 y)
Dermawan et al ⁴	Male	77	LLL	3.9	<i>YAP1</i> (exon 4):: <i>TFE3</i> (exon 7)	ANED (7 mo)
	Male	35	RML	7.5	<i>YAP1</i> (exon 4):: <i>TFE3</i> (exon 7)	ANED (6 mo)
Zhang et al ⁷	Female	40	LLL	0.9	<i>TFE3</i> FISH negative for translocation	ANED (3 mo)
Dehner et al ⁵	Female	24	Bilateral	5.8	<i>YAP1</i> (exon 4):: <i>TFE3</i> (exon 7)	DOD (7 mo)
	Female	55	LUL	9.5	<i>YAP1</i> (exon 4):: <i>TFE3</i> (exon 7)	ANED (43 mo)
	Female	66	RML	2.9	<i>YAP1</i> (exon 4):: <i>TFE3</i> (exon 7)	NA
	Female	69	RLL	1.0	<i>YAP1</i> (exon 4):: <i>TFE3</i> (exon 7)	NA
Jaksa et al ⁶	Male	57	RUL	4.5	<i>YAP1</i> (exon 4):: <i>TFE3</i> (exon 7)	ANED (12 mo)
Current study (previously unpublished cases)	Male	42	LLL	2.3	<i>YAP1</i> (exon 4):: <i>TFE3</i> (exon 7)	ANED (104 mo)
	Female	56	RL	NA	<i>YAP1</i> (exon 4):: <i>TFE3</i> (exon 7)	NA
	Male	63	RLL	2.0	<i>YAP1</i> (exon 4):: <i>TFE3</i> (exon 7)	ANED (3 mo)
	Female	84	LLL	5.5	<i>YAP1</i> (exon 4):: <i>TFE3</i> (exon 7)	ANED (18 mo)
	Female	61	RLL	0.7	<i>YAP1</i> (exon 4):: <i>TFE3</i> (exon 7)	ANED (3 mo)
	Male	41	RUL	3.4	<i>TFE3</i> rearrangement	ANED (22 mo)
Summary	Male: 8 (32%)	Median: 55	RUL: 5	Median: 2.8	Breakpoints of fusion-positive cases:	ANED: 17/19
	Female: 17 (68%)	Range: 24-84	RML: 2	Range: 0.7-9.5	<i>YAP1</i> (exon 4):: <i>TFE3</i> (exon 7): 14/15 (93%)	AWD: 1/19
			LLL: 4		<i>YAP1</i> (exon 5):: <i>TFE3</i> (intron 6): 1/15 (7%)	DOD: 1/19
			RL: 1			
			LUL: 4			
			LLL: 6			
			LMB: 1			
			Bilateral: 1			

ANED, alive with no evidence of disease; AWD, alive with disease; DOD, died of disease; FISH, fluorescence in situ hybridization; LLL, left lower lobe; LMB, left main bronchus; LUL, left upper lobe; NA, not available; RL, right lung; RLL, right lower lobe; RML, right middle lobe; RNAseq, RNA sequencing; RUL, right upper lobe.

detected using FISH or inferred with IHC. IMT is negative for *TFE3*.

The presence of an inflammatory infiltrate could also suggest AFH. In AFH, lymphocytes and plasma cells are usually present in peripheral aggregates, as can be seen in CCST. However, the tumor cells have more eosinophilic cytoplasm, and areas of hemorrhage or blood-filled cystic spaces are often present. Based on IHC, AFH may express EMA, desmin, and/or CD99, whereas *TFE3* is negative. At the molecular level, AFH most commonly harbors an *EWSR1*::*CREB1* gene fusion, whereas alternative fusions (*EWSR1*::*ATF1* and *FUS*::*ATF1*) are also recognized.

Follicular dendritic cell sarcoma (FDSC) is an uncommon neoplasm that usually affects lymph nodes, although rare pulmonary cases have been described.²¹ It is typically composed of spindle- to ovoid-shaped cells with pale eosinophilic cytoplasm and nuclei with open chromatin and variably prominent nucleoli. A prominent lymphocytic infiltrate is usually present, a feature that is shared by most examples of CCST. Based on IHC, however, FDSC is typically positive for CD21, CD23, and/or CD35. Unlike

CCST, FDSC is not known to harbor recurrent gene fusions. Instead, sequencing studies have identified recurrent alterations in the nuclear factor kappa-light-chain-enhancer of activated B cells pathway.²²

Entrapment of normal respiratory epithelium by the CCST cells can impart a biphasic appearance. Coupled with well-defined delineation on imaging and gross, these features can mimic sclerosing pneumocytoma. In addition, sclerosing pneumocytomas can also display prominent vascularity with cystic hemorrhagic spaces. Again, in challenging cases, IHC can readily differentiate between the 2 entities. Sclerosing pneumocytomas typically express keratins (eg, CAM5.2 and CK7) and Napsin A in the epithelial component only, and TTF1 and EMA in both stromal and epithelial components. Anecdotally, keratin positivity can be seen in both components. Finally, pulmonary carcinoid tumors often demonstrate similar clinical presentation, with a well-defined appearance on imaging and a frequent association with airways. By virtue of their vastly diverse cytologic and architectural appearances as well as relative frequency, they can be considered on the

differential with CCST. These tumors can display similar histologic features, including clearing of the cytoplasm, a spindle-to-ovoid cell shape, vaguely nested growth patterns, prominent vascularization, and entrapment of the respiratory epithelium. Unlike CCST, pulmonary carcinoid tumors tend to display more regular nuclear contours and characteristic finely granular ("salt and pepper") chromatin. None of the reported cases of CCST demonstrated expression of neuroendocrine markers.

In conclusion, we report the clinical, histologic, immunophenotypic, and molecular characteristics of the largest series of CCST of the lung. CCST demonstrates distinctive morphologic, genomic, and clinical features. Although rare cases with aggressive behavior have been reported previously elsewhere, all cases with available clinical follow-up in our study pursued an indolent clinical course with no recurrences or metastases. Genomically, most tumors demonstrate consistent *YAP1* exon 4::*TFE3* exon 7 fusion. Although CCST did not exhibit any markers supporting a specific line of differentiation, we show that IHC for *YAP1*-CT and *TFE3* can be used as surrogate markers to identify fusion-positive cases. Our findings support wider recognition of this novel entity.

Acknowledgments

The authors gratefully acknowledge the following pathologists and clinicians who kindly provided case material and clinical follow-up information, where available: Dr Kumarasen Cooper (Burlington, VT), Dr Bernadette Liegl-Atzwanger (Graz, Austria), Dr Kossivi Dantey (Pittsburgh, PA), Dr David Harrison (Quincy, MA), Dr Angela J. Tate (St. John's, Canada), and Dr Cunxian Zhang (Warwick, RI). The authors would like to thank Dr Azra Ligon from Brigham and Women's Hospital for her valuable assistance with interpretation of *TFE3* fluorescence *in situ* hybridization.

Author Contributions

I.O. and W.J.A. conceived and designed the study, acquired and analyzed the data, and wrote and reviewed the manuscript. A.I., K.J.F., Y.P.H., and P.K. provided material support. C.D.M.F. reviewed the study concept and design and provided material support. L.M.S. performed analysis of the molecular results. All authors read, reviewed, and approved the final manuscript.

Data Availability

All data generated or analyzed during this study are included in this published article and its supplementary files. The authors can provide any additional data upon reasonable request.

Funding

This work was supported by academic funds from the Department of Pathology at Brigham and Women's Hospital.

Declaration of Competing Interest

The authors have no conflicts of interest to disclose.

Ethics Approval and Consent to Participate

This study was approved by the Institutional Review Board of Mass General Brigham (protocol number: 2023P002089).

Supplementary Material

The online version contains supplementary material available at <https://doi.org/10.1016/j.modpat.2024.100632>.

References

1. Falconeri G, Mirra M, Michal M, Suster S. Hemangioblastoma-like clear cell stromal tumor of the lung. *Adv Anat Pathol*. 2013;20(2):130–135. <https://doi.org/10.1097/PAP.0b013e318286245d>
2. Lindholm KE, Moran CA. Hemangioblastoma-like clear cell stromal tumor of the lung: a clinicopathologic and immunohistochemical study of 5 cases. *Am J Surg Pathol*. 2020;44(6):771–775. <https://doi.org/10.1097/PAS.0000000000001429>
3. Agaimy A, Stoehr R, Michal M, et al. Recurrent *YAP1*-*TFE3* gene fusions in clear cell stromal tumor of the lung. *Am J Surg Pathol*. 2021;45(11):1541–1549. <https://doi.org/10.1097/PAS.0000000000001719>
4. Dermawan JK, Azzato EM, McKenney JK, Liegl-Atzwanger B, Rubin BP. *YAP1*-*TFE3* gene fusion variant in clear cell stromal tumour of lung: report of two cases in support of a distinct entity. *Histopathology*. 2021;79(6):940–946. <https://doi.org/10.1111/his.14437>
5. Dehner CA, Sadeghi D, Boulos F, et al. Clear cell stromal tumour of the lung with *YAP1*::*TFE3* fusion: four cases including a case with highly aggressive clinical course. *Histopathology*. 2022;81(2):239–245. <https://doi.org/10.1111/his.14706>
6. Jakša R, Stržinská I, Kendall Bártu M, Trča S, Matěj R, Dundr P. Clear cell stromal tumor of the lung with multinucleated giant cells: a report of a case with *YAP1*-*TFE3* fusion. *Diagn Pathol*. 2023;18(1):9. <https://doi.org/10.1186/s13000-023-01304-0>
7. Zhang X, Huang B, Jiang H, Wei H. Case report: hemangioblastoma-like clear cell stromal tumor of the left lower lung. *Front Med (Lausanne)*. 2022;9:836012. <https://doi.org/10.3389/fmed.2022.836012>
8. Sharain RF, Gowin AM, Greipp PT, Folpe AL. Immunohistochemistry for *TFE3* lacks specificity and sensitivity in the diagnosis of *TFE3*-rearranged neoplasms: a comparative, 2-laboratory study. *Hum Pathol*. 2019;87:65–74. <https://doi.org/10.1016/j.humpath.2019.02.008>
9. Anderson WJ, Fletcher CDM, Hornick JL. Loss of expression of *YAP1* C-terminus as an ancillary marker for epithelioid hemangioendothelioma variant with *YAP1*-*TFE3* fusion and other *YAP1*-related vascular neoplasms. *Mod Pathol*. 2021;34(11):2036–2042. <https://doi.org/10.1038/s41379-021-00854-2>
10. Russell-Goldman E, Hornick JL, Hanna J. Utility of *YAP1* and *NUT* immunohistochemistry in the diagnosis of porocarcinoma. *J Cutan Pathol*. 2021;48(3):403–410. <https://doi.org/10.1111/cup.13924>
11. Garcia EP, Minkovsky A, Jia Y, et al. Validation of OncoPanel: a targeted next-generation sequencing assay for the detection of somatic variants in cancer. *Arch Pathol Lab Med*. 2017;141(6):751–758. <https://doi.org/10.5858/arpa.2016-0527-OA>
12. Zheng Z, Liebers M, Zhelyazkova B, et al. Anchored multiplex PCR for targeted next-generation sequencing. *Nat Med*. 2014;20(12):1479–1484. <https://doi.org/10.1038/nm.3729>
13. Robinson JT, Thorvaldsdóttir H, Winckler W, et al. Integrative genomics viewer. *Nat Biotechnol*. 2011;29(1):24–26. <https://doi.org/10.1038/nbt.1754>
14. Dermawan JK, Azzato EM, Billings SD, et al. *YAP1*-*TFE3*-fused hemangiendothelioma: a multi-institutional clinicopathologic study of 24 genetically-confirmed cases. *Mod Pathol*. 2021;34(12):2211–2221. <https://doi.org/10.1038/s41379-021-00879-7>
15. Zhao B, Wei X, Li W, et al. Inactivation of *YAP* oncprotein by the Hippo pathway is involved in cell contact inhibition and tissue growth control. *Genes Dev*. 2007;21(21):2747–2761. <https://doi.org/10.1101/gad.1602907>
16. Di Malta C, Zampelli A, Granieri L, et al. *TFEB* and *TFE3* drive kidney cystogenesis and tumorigenesis. *EMBO Mol Med*. 2023;15(5):e16877. <https://doi.org/10.1522/emmm.202216877>
17. Settembre C, Zoncu R, Medina DL, et al. A lysosome-to-nucleus signalling mechanism senses and regulates the lysosome via mTOR and *TFEB*. *EMBO J*. 2012;31(5):1095–1108. <https://doi.org/10.1038/embj.2012.32>
18. Akumalla S, Madison R, Lin DI, et al. Characterization of clinical cases of malignant PEComa via comprehensive genomic profiling of DNA and RNA. *Oncology*. 2020;98(12):905–912. <https://doi.org/10.1159/000510241>
19. Lu L, Drew PA, Yachnis AT. Hemangioblastoma in the lung: metastatic or primary lesions? *Case Rep Pathol*. 2014;2014:468671. <https://doi.org/10.1155/2014/468671>
20. Argani P, Gross JM, Baraban E, et al. *TFE3* - rearranged PEComa/PEComa-like neoplasms: report of 25 new cases expanding the clinicopathologic spectrum and highlighting its association with prior exposure to chemotherapy. *Am J Surg Pathol*. 2024;48(7):777–789. <https://doi.org/10.1097/PAS.00000000000002218>
21. Hollingsworth J, Cooper WA, Nicoll KD, et al. Follicular dendritic cell sarcoma of the lung: a report of two cases highlighting its pathological features and diagnostic pitfalls. *Pathology*. 2011;43(1):67–70.
22. Griffin GK, Sholl LM, Lindeman NI, Fletcher CDM, Hornick JL. Targeted genomic sequencing of follicular dendritic cell sarcoma reveals recurrent alterations in NF-κB regulatory genes. *Mod Pathol*. 2016;29(1):67–74.